applied sciences

MDPI

Article

A Novel Wideband Common-Mode Noise Suppression Filter That Combines Mushroom and Defected Corrugated Reference Plane Structures

Chung-Ke Yu [1], Ding-Bing Lin [2,*] and Hsin-Piao Lin [1]

[1] Department of Electronic Engineering, National Taipei University of Technology, Taipei 10608, Taiwan
[2] Department of Electronic and Computer Engineering, National Taiwan University of Science and Technology, Taipei 10607, Taiwan
* Correspondence: dblin@mail.ntust.edu.tw

Abstract: A novel wideband common-mode (CM) suppression filter is proposed for high-speed transmission. The filter is embedded in 3 10 mm × 10 mm layers of a printed circuit board (PCB) that combines a mushroom structure and a defected corrugated reference plane structure (MDCRP). Using the novel MDCRP structure generates more resonance frequencies in the CM current return path. This generates a wider CM noise suppression performance. We used a simulation method to obtain the best geometric parameters for the MDCRP structure. The experimental results proved that the full-wave simulation results were consistent with the actual measurement results. This novel filter shows good signal integrity according to actual measurements, and the insertion loss can be kept to less than −2.306 dB from DC to 21 GHz in differential mode (DM). The CM noise can be suppressed by over −10 dB from 5.09 GHz to 20.62 GHz. The fractional bandwidth is 120.8%, and the CM noise improves by 64.5%. An eye diagram proves that the filter can support a 20 Gb/s transmission rate with complete differential signal transmission capability. The MDCRP structure filter can support HDMI 2.0, PCI Express 4.0, USB 3.2, and SATA Express. Therefore, the filter meets current computer and server system products' design needs.

Keywords: common-mode noise; differential signal; electromagnetic interference; mushroom structure; signal integrity

check for updates

Citation: Yu, C.-K.; Lin, D.-B.; Lin, H.-P. A Novel Wideband Common-Mode Noise Suppression Filter That Combines Mushroom and Defected Corrugated Reference Plane Structures. *Appl. Sci.* **2023**, *13*, 4616. https://doi.org/10.3390/app13074616

Academic Editors: Giuseppe Lacidogna and Lamberto Tronchin

Received: 1 February 2023
Revised: 29 March 2023
Accepted: 31 March 2023
Published: 5 April 2023

Copyright: © 2023 by the authors. Licensee MDPI, Basel, Switzerland. This article is an open access article distributed under the terms and conditions of the Creative Commons Attribution (CC BY) license (https://creativecommons.org/licenses/by/4.0/).

1. Introduction

In today's computer product market, the processing speed of systems is becoming faster and faster, so the related interface speed of computer peripheral devices must also be increased accordingly, which means increasing the data transmission rate. For example, HDMI 2.0 requires a transmission rate of 18 Gb/s, PCI Express 4.0 requires a transmission rate of 16 Gb/s, USB 3.2 requires a transmission rate of 10 Gb/s, and SATA Express requires a transmission rate of 16 Gb/s. In computer design, differential signaling is often used to increase the transmission rate and has the characteristics of low crosstalk, strong antinoise, and low electromagnetic interference (EMI) [1]. Differential signaling is used to design high-speed digital buses that dramatically reduce common-mode noise, which allows higher data rates to be realized. Differential signaling has a virtual reference plane that provides a continuous return path for the current [2]. Differential signaling requires proper termination of the differential impedance between the two traces. The two transmission lines must also be of equal length and must be routed parallel to each other to avoid creating serious electromagnetic interference (EMI) problems. Layer jumps must be avoided as they cause impedance discontinuity and reflections. The same number of vias needs to exist between the two signal pairs to avoid distorting the signal integrity [3].

PCB layout design is difficult to improve due to its high-density component layout and compact size. Improvements must consider the PCB geometry, trace length, spacing,

thickness, and via design to reduce reflection and signal attenuation [4]. In a microstrip configuration, the high-frequency return current follows the path of least inductance back to the source. In the case of plane splitting or layer transitions to different references, the return current is forced to deviate from the ideal path. Non-ideal return paths can also generate CM currents, adding to EMI problems [5]. Bending and asymmetrical traces due to component arrangement in dense PCB layouts cause unwanted CM noise and signal integrity issues, which can lead to severe EMI issues [6]. Many CM filter designs involving defected ground structure (DGS) and mushroom-like structures have been published, which were to solve the related CM noise problems. In these DGS structural papers, a double-slit complementary split ring resonator (S-DBCSRR) structure filter has etched a slot to support the highest rejection frequency of 4.07 GHz [7]. A DGS structure filter used 2 enhanced coupled C-shapes to achieve the highest suppression frequency of 10.8 GHz [8]. Adding 3 varactor-loaded into a DGS structure filter achieved the highest suppression frequency of 8.1 GHz [9]. Using 5 DGS units to become a dual-resonant function filter achieved the highest suppression frequency of 4.6 GHz [10]. These DGS structures have been studied in the literature, and they can only support a suppression frequency of up to 10.8 GHz, so they cannot support today's computer design requirements.

Mushroom-like structures with different structural changes and noise suppression capabilities have been studied in the literature. For example, a 4-mushroom structure for a filter using negative permittivity metamaterials achieved the highest suppression frequency of 7.1 GHz [11]. Using a pair of meandered lines and a mushroom-like structure filter achieved the highest rejection frequency of 5.2 GHz [12]. The filter uses a quarter-wavelength resonator to support the highest suppression frequency of 10.1 GHz [13]. A filter that combined a pair of meandered lines and multi-layer mushroom-like structures achieved the highest rejection frequency of 13.41 GHz [14]. A combination of a serpentine transmission line and a ring structure filter achieved the highest suppression frequency of 7.87 GHz [15].

The periodically corrugated reference plane (PCRP)-structured filter achieved the highest rejection frequency of 10.4 GHz [16]. These mushroom-like and PCRP structure literature results only achieve the highest rejection frequency of 13.41 GHz, which cannot meet the suppression frequency of 18 GHz to support the current high-speed buses in computer products. In addition, using the defected corrugated reference plane (DCRP) structure filter achieved the highest suppression frequency of 17.03 GHz, which can support the requirements of PCI Express 4.0, SATA Express, and USB 3.2, but not that of HDMI 2.0 [17].

Computer and consumer electronic products are experiencing increasing demand for high-quality multimedia transmission. High-definition multimedia interface (HDMI) is used in video and audio transmission and reaches a maximum transmission rate of 18 Gb/s. The main aim of this paper is to design a filter capable of supporting high-speed buses at 20 Gb/s, enabling it to support buses of HDMI 2.0, PCI Express 4.0, and SATA Express. Because the highest suppression frequency of a DCRP structure filter cannot reach 18 GHz, it cannot support the requirements of HDMI 2.0. Therefore, this paper uses a mushroom structure added into a DCRP structure to increase the suppression frequency. The structure change generates characteristic impedances change in the CM current return path resulting in different resonance frequencies for a wider stopband effect. This improves the noise suppression ability at higher frequencies, making it a novel broadband CM noise suppression filter that uses an MDCRP structure to support HDMI 2.0.

2. Common-Mode Noise Suppression Filter Design

The MDCRP structure filter design uses a PCB material of TU-933 (ε_r = 3.09, tanδ = 0.002) for high frequency, from the Taiwan Union Technology Corporation (TUC) to support up to 20 GHz. The filter dimension is 10 mm × 10 mm of a 4-layer PCB. A three-dimensional view of the MDCRP structure filter is shown in Figure 1a. There are 2 coupled microstrip lines on the top layer, and the trace width, length, and spacing between the

2 coupled lines in the differential pair are 0.163 mm, 10 mm, and 0.3 mm, respectively. There are two ground planes and a mushroom structure under the two coupled lines of a differential pair. There are eight vias to connect two ground planes, and there are two vias to connect the mushroom structure and second ground planes that form the MDCRP structure filter. The via side view is shown in Figure 1b. The total thickness of the PCB is 0.77 mm, which can be divided into 4 metal layers (T1, T2, T3, and T4) and 3 insulating layers (H1, H2, and H3). There are differential pairs and via pads in layer 1 (T1), the first ground plane is in layer 2 (T2), the second ground plane is in layer 3 (T3), and there are only via pads in layer 4 (T4). The via diameter is 0.2 mm, the via pad diameter is 0.406 mm, and all vias traverse every layer of the PCB. The entire filter only uses three PCB board layers.

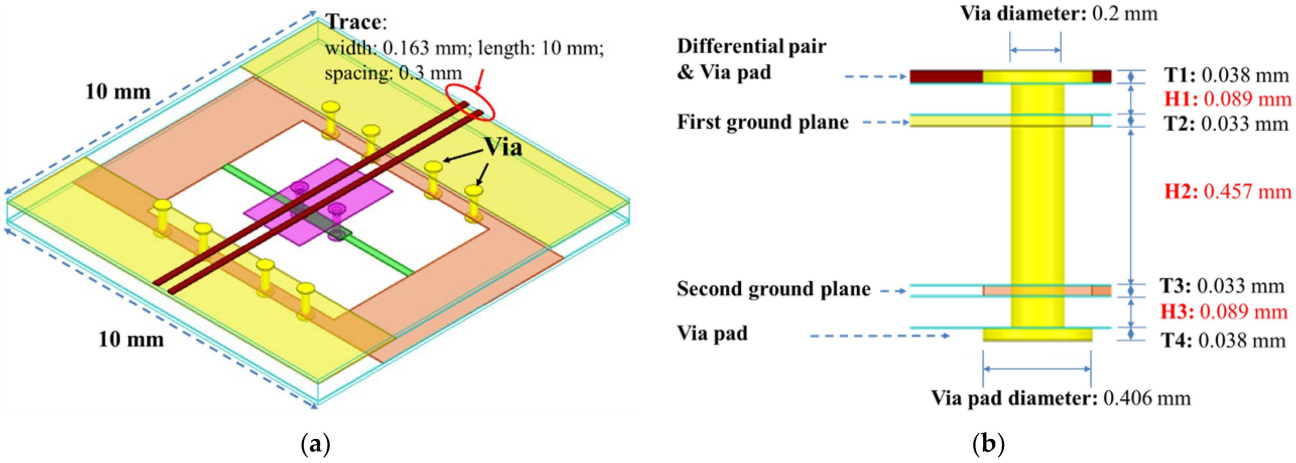


Figure 1. The proposed MDCRP filter structure. (**a**) Three-dimensional view. (**b**) Via side view.

The first ground plane is shown in Figure 2a. It cuts a 5 mm × 10 mm slot to become the 2 ground sheets for GL1a and GL1b. The GL1a and GL1b of the ground sheet is connected to the second ground using four vias, respectively. There is a 3 mm × 1.8 mm mushroom sheet between the GL1a ground sheet and the GL1b ground sheet, which uses 2 vias to connect the second ground plane. The second ground plane is shown in Figure 2b. The size is 5.8 mm × 10 mm. There are two opposite C-shaped slots on the second ground plane. There are four vias on each side connected to the GL1a ground sheet and the GL1b ground sheet, respectively, and there are two vias connected to the mushroom sheet in the middle. These structural changes give us an MDCRP structure filter. The relevant dimensions in the first and second ground planes are shown in Table 1.

Table 1. The geometric parameters of the MDCRP structure filter.

Parameter	**GL1a**	**GL1b**	**GW1**	**SL1**	**SW1**	**ML**
Length (mm)	2.5	2.5	10	5	10	3
Parameter	**MW**	**GL2**	**GW2**	**SL2**	**SW2**	**LL1**
Length (mm)	1.8	5.8	10	5	6	2.1
Parameter	**LW1**	**LL2**	**LW2**	**LL3**	**LW3**	**—**
Length (mm)	0.2	1.8	0.4	2.1	0.2	—

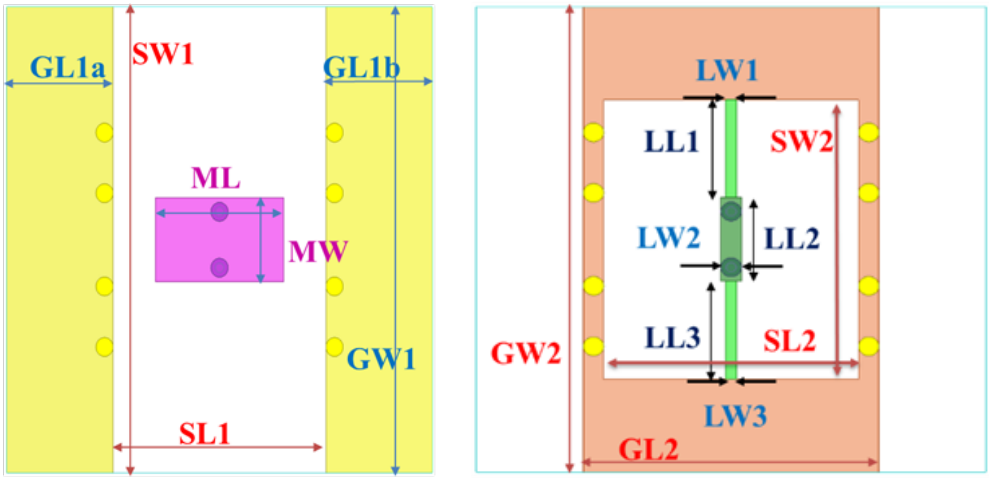


Figure 2. The proposed MDCRP structure filter. (**a**) The first ground plane. (**b**) The second ground plane.

2.1. Design Concept of Filter

The very tight layout of the components of the PCB design often causes the path of the differential signal to be asymmetrical, which generates a lot of CM noise. A CM noise suppression filter is required to solve this problem. The MDCRP structure filter's design concept utilizes the differential signaling principle, the stepped impedance characteristics, and the CM return current path. Adding a mushroom structure to the defective corrugated reference plane structure creates multiple different CM current return paths.

The differential signal has a virtual reference ground, which does not affect the differential signal transmission when the reference ground is damaged. However, the CM signal has a great impact because the CM signal current uses the ground plane to return to the source. The slot in the first ground plane blocks the CM current and allows it to flow smoothly through the via to the second ground plane. The mushroom structure of the first ground plane also allows the CM current to flow smoothly to the second ground plane. The second ground plane is the DGS structure, which changes the CM current return path. This results in several resonance points and many approach transmission zeros, which generate a wider suppression bandwidth, and maintains the signal integrity when the transmission is in DM.

The side view of the CM current return path of the differential pair transmission of the PCB is shown in Figure 3. The differential pair is in layer 1 of the PCB, and the ground planes are in layers 2 and 3, respectively. The CM current return path passes through the first ground plane on the right (GL1b), through the four vias on the right to the second ground plane (GL2), and then through the four vias on the left to reach the first ground plane on the left (GL1a), forming a current return path. There is another current return path through the mushroom structure that passes through two vias to the second ground plane (GL2) and then passes through the four vias on the left to the first ground plane on the left (GL1a). Using the MDCRP structure creates more resonance points, which generate a broadband CM noise suppression capability to avoid EMI problems.

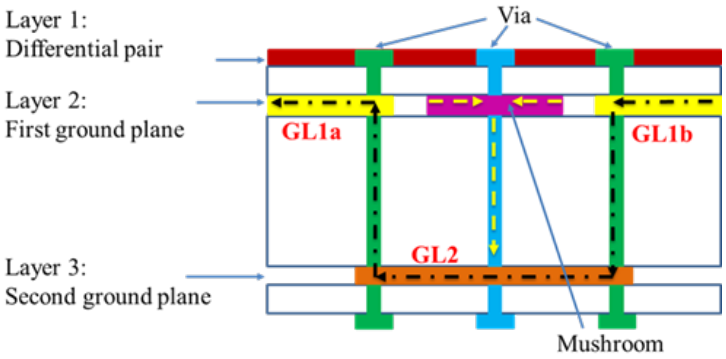


Figure 3. The CM current return path of the differential pair transmission signal.

2.2. Geometric Parameter Design of Filter

We used ANSYS HFSS software to identify the MDCRP structure filter's related geometric parameters for simulation and analysis. This allowed us to observe the CM insertion loss (S_{cc21}) under parameter performance changes and the CM rejection effect's impact.

The effect of the length of slot 2 (SL2) is shown in Figure 4a. The SL2 in the second ground plane is modified to be 2 mm, 3 mm, 4 mm, and 5 mm, respectively. The CM noise suppression performance widens when the SL2 is longer. The suitable choice is 5 mm for SL2, which achieves a better rejection effect.

The effect of the width of Slot 2 (SW2) is shown in Figure 4b. The SW2 in the second ground plane is modified to be 4 mm, 6 mm, 8 mm, and 9.6 mm, respectively. The CM noise suppression performance improves when SW2 is narrower. The suitable choice is 6 mm for SW2, which results in a wider stopband performance.

The effect of the via quantity (VQ) is shown in Figure 4c. The VQ is modified to be 2 pcs, 4 pcs, 6 pcs, and 8 pcs, respectively. The VQ is increased to improve the CM noise suppression performance, and the stopband performance moves toward a high-frequency location. The most suitable choice is 8 pcs of vias, which achieves better stopband performance.

The effect of the mushroom length (ML) is shown in Figure 4d. The ML in the first ground plane is modified to be 2 mm, 3 mm, 4 mm, and 4.8 mm, respectively. The CM noise stopband performance moves toward a low-frequency location when the ML is longer. The most suitable choice is 3 mm for ML, which achieves a wider stopband effect.

The effect of the mushroom width (MW) is shown in Figure 4e. The MW in the first ground plane is modified to be 1.8 mm, 2.4 mm, 3 mm, and 3.6 mm, respectively. The CM noise stopband performance of the high-frequency range improves when the MW is narrower. The most suitable choice is 1.8 mm of MW, which results in a wider stopband performance.

The CM insertion loss (S_{cc21}) parameter results prove that changes in the geometric parameters of the MDCRP structure filter generate more resonance points to achieve a wider suppression bandwidth, which proves that the geometric parameter change results are consistent with the theory.

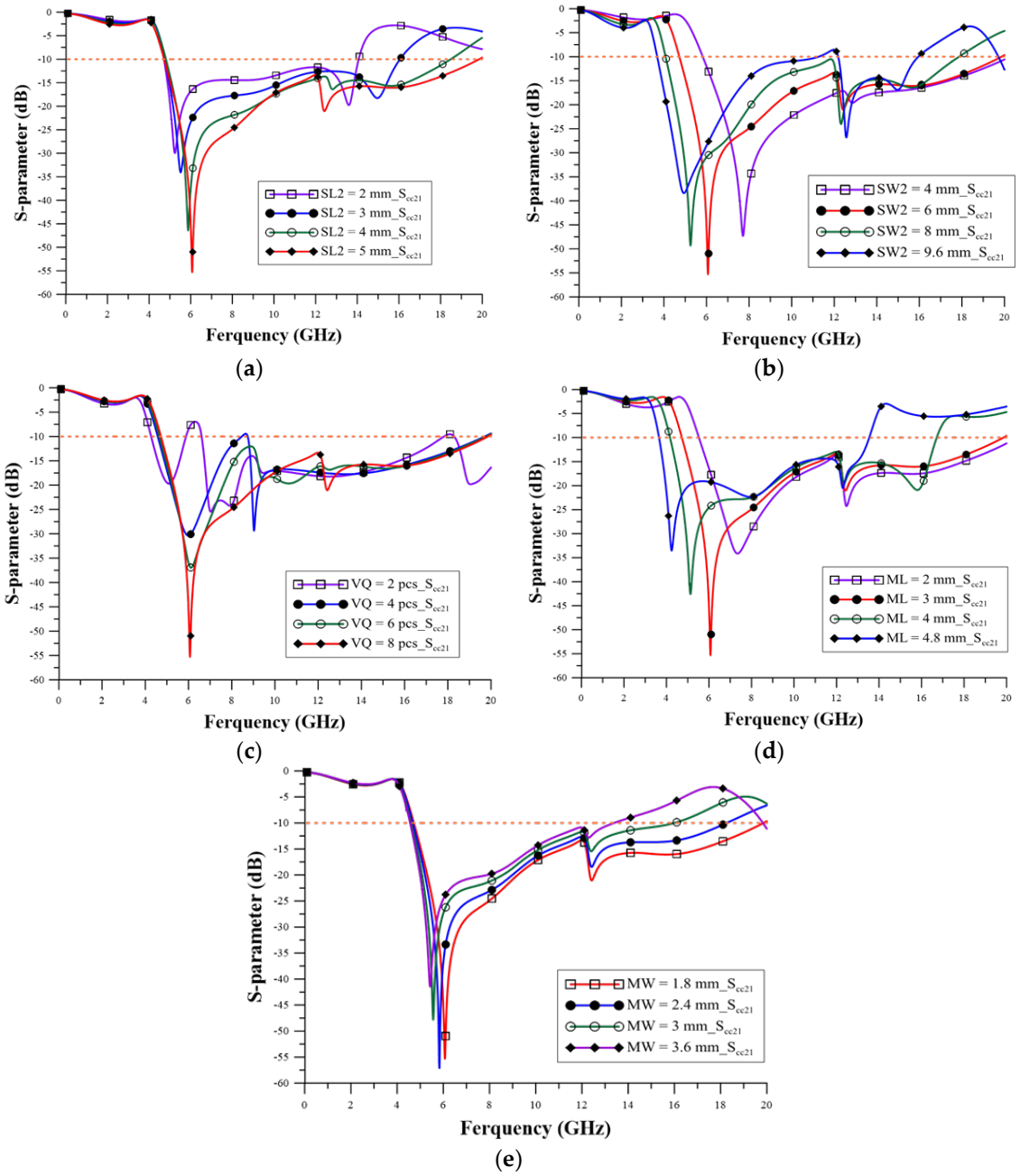


Figure 4. The effect of the geometric parameter changes of the MDCRP filter on the CM insertion loss. (**a**) The length of slot 2 (SL2). (**b**) The width of slot 2 (SW2). (**c**) Via quantity (VQ). (**d**) Mushroom length (ML). (**e**) Mushroom width (MW).

2.3. Equivalent Circuit Model

The equivalent circuit modeling involves the observation and theoretical derivation of the MDCRP filter structure. The side view of the MDCRP structure filter is shown in Figure 5a, in which we can observe the mushroom and DCRP structures. The microstrip line can be divided into five parts where two parts cannot refer to the first ground plane, forming two equivalent inductances of L1 and L2. The two ends of L1 and L2 become equivalent C1, C2, C3, and C4 capacitances with the first ground and mushroom ground planes, and the other three parts are the equivalent models of the coupled microstrip lines of CML1, CML2, and CML3. The two vias in the mushroom structure become the equivalent inductance of L5, which connects the second ground plane. The four vias on the left connect

to the second ground plane to become the equivalent inductance of L3. The four vias on the right connect to the second ground plane to become the equivalent inductance of L4.

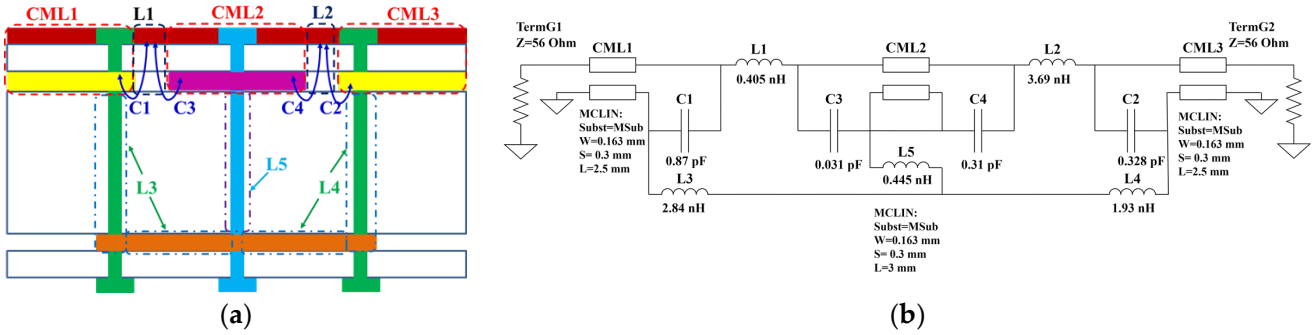


Figure 5. (**a**) The MDCRP structure filter side view. (**b**) Equivalent half-circuit model.

The equivalent half-circuit model is shown in Figure 5b. Then, we imported all the relevant PCB and microstrip line parameters into the equivalent circuit model of the Advanced Design System (ADS) for simulation, this produces CM insertion loss (S_{cc21}) parameters. The equivalent components (L1, L2, L3, L4, L5, C1, C2, C3, and C4) were adjusted to achieve CM insertion loss (S_{cc21}) parameters similar to a simulation result, allowing these equivalent components to be effective parameters.

We modified equivalent component parameters to cause the CM insertion loss (S_{cc21}) parameter change. When the larger value of L1 has better suppression of low-frequency CM noise, the larger value of L2 has worse suppression of CM noise, affecting the resonance frequency change in the low-frequency band. When the value of L3 is larger, the suppression of CM noise in the low-frequency band is worse, and the suppression of CM noise in the high-frequency band is better. A smaller L4 value affects the resonant frequency change in the low-frequency band. When the value of L5 is smaller, it affects the resonance frequency change in the low-frequency band, and the suppression of CM noise in the low-frequency band is worse.

When the value of C1 is smaller, it affects the change in resonance frequency in the low-frequency band, and the suppression of CM noise is worse. When the value of C2 is smaller, it affects the change in resonance frequency in the low-frequency band, and the suppression of CM noise is worse. When the value of C3 is smaller, the suppression of CM noise in the high-frequency band is better, but the suppression of CM noise in the low-frequency band is worse. When the value of C4 is smaller, the suppression of CM noise in the high-frequency band is better, but the suppression of CM noise in the low-frequency band is worse and shifts toward low frequencies.

A verification equivalent half-circuit model by full-wave simulation of the CM insertion loss is shown in Figure 6. The CM insertion loss (S_{cc21}) parameters of both are very similar. The suppression bandwidths are also very similar, which proves the validity of the equivalent circuit model.

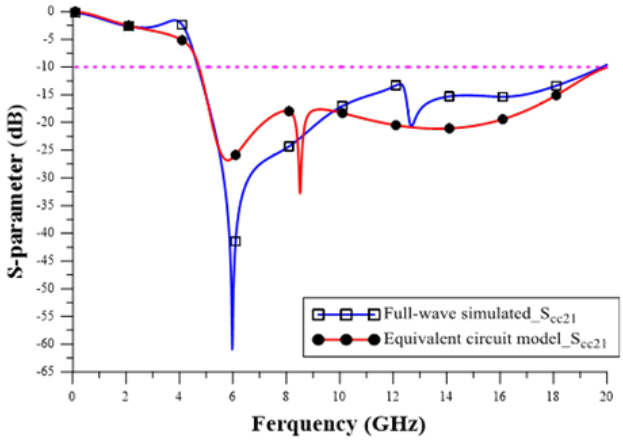


Figure 6. Verification equivalent half-circuit model by full-wave simulation of the CM insertion loss.

3. Experimental Results

The MDCRP structure filter verified the suppression bandwidth of CM noise through real measurements. Therefore, the entire filter used 4 layers of TU-933 PCB material to facilitate measurements with a filter size of 60 mm × 50 mm, but the filter structure only used a 3-layer PCB.

We measured the related mixed-mode scattering parameters by a PNA Network Analyzer N5227A (Agilent Technologies, Santa Clara, CA, USA). PCB photos of the top and bottom view for the reference board are shown in Figure 7a, which shows that it maintains a complete ground plane. We used a physical layer test system (PLTS) (Keysight Technologies, Santa Rosa, CA, USA) of automatic fixture removal (AFR) calibration technology, which achieves the true measurement of the device under test (DUT) to reduce the relative measurement errors. PCB photos of the top and bottom views of the MDCRP structure filter board are shown in Figure 7c.

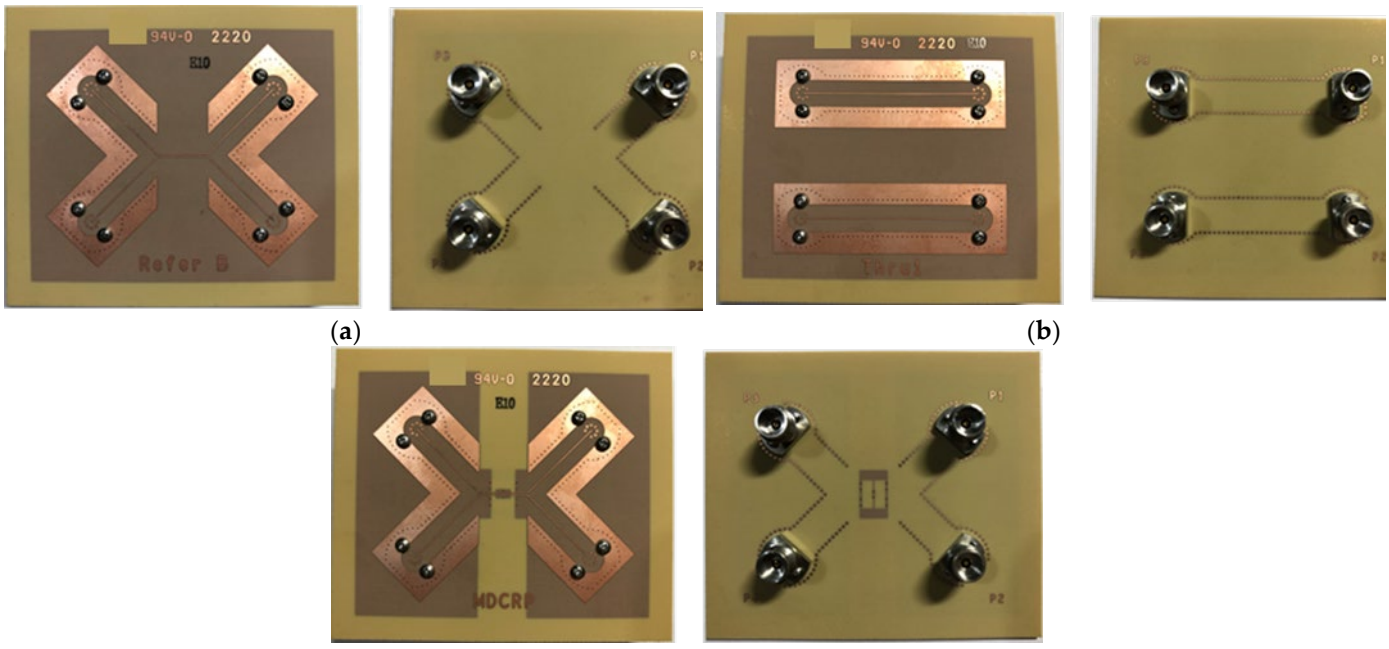


Figure 7. Photos of the measured PCB structure. (**a**) The reference boards. (**b**) The 2× through the board. (**c**) The MDCRP structure filter board.

3.1. Frequency Domain Analysis

A comparison of simulated and measured DM insertion loss (S_{dd21}) results is shown in Figure 8. The DM insertion loss in the range from DC to 21 GHz range was kept below −2.183 dB in the simulated results. The measured results used the AFR process to achieve more accurate values, and the DM insertion loss in the range from DC to 21 GHz range was kept below −2.306 dB, which proves that the MDCRP structure filter has good signal integrity in DM.

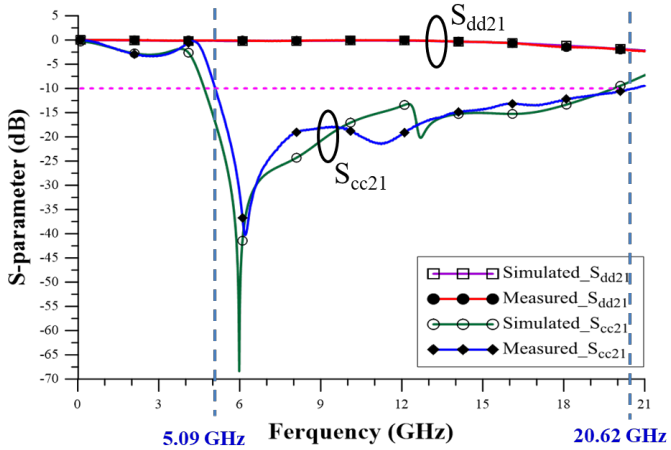


Figure 8. Comparison of simulated and measured insertion loss results.

In addition, a comparison of simulated and measured CM insertion loss (S_{cc21}) results are shown in Figure 8. In the simulated results, the CM noise can be reduced by over 10 dB from 4.69 GHz to 19.82 GHz, the fractional bandwidth was 123.5%, and the center frequency was 12.25 GHz. To obtain more accurate measurement values through AFR technology, in the measured experiment, the CM noise was reduced by over 10 dB from 5.09 GHz to 20.62 GHz, the fractional bandwidth was 120.8%, and the center frequency was 12.85 GHz. The measurement of the suppression bandwidth was somewhat different in the simulated results, where it shifted to high-frequency areas, resulting in poorer fractional bandwidth. It can be observed that there is a difference in the CM insertion loss (S_{cc21}) for 10 dB between the simulation results and the measurement results because of PCB manufacturing errors and the inductance characteristics of the via, which are very difficult to control in the manufacturing process. This results in resonant frequency changes, so the measurement results do not match the simulation results unanimously. The fact that the different parts in both can be kept below −10 dB proves that the filter has a good CM noise rejection effect. The CM characteristics indicate that the actual measured results show 3 resonance frequencies, which are 6.20 GHz, 11.24 GHz, and 17.07 GHz, respectively. The MDCRP structure filter shows wideband CM noise suppression and good signal integrity.

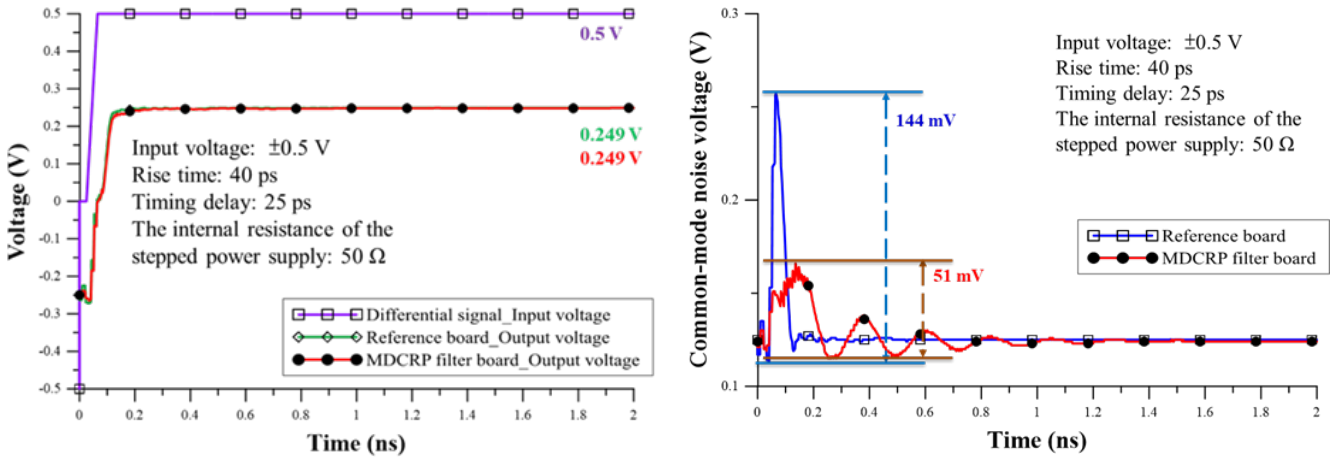
3.2. Time Domain Analysis

We generated S4P files for the MDCRP structure filter board and the reference board using the measurement results. These S4P files were inputted into ADS schematic tools for the simulation, which set the related parameters. The input terminals were fed with ±0.5 V, the rise time was 40 ps, the timing delay was 25 ps, and the internal resistance of the power supply was a stepped power supply of 50 Ω. Equations (1) and (2) were used to calculate the DM voltage of the output and the CM noise voltage of the output in the time domain transmission (TDT). We compared the MDCRP structure filter board and the reference board in actual measurement results.

$$V_{TDT-differential} = V_+ - V_- \quad (1)$$

$$V_{TDT-common} = \frac{V_+ + V_-}{2} \quad (2)$$

The DM output voltage in the TDT is shown in Figure 9a. It can be seen that the final input voltage is 0.5 V. The actual input voltage is divided into 2.5 V through the internal resistance of the power supply and the terminal impedance, which are the inputs to the MDCRP structure filter board and the reference board. The MDCRP structure filter board was compared with the reference board, and we observed that the DM signals of the output were very similar at 0.249 V. The latency times were also very similar. This proves that the MDCRP structure filter does not influence the quality of the DM signal and maintains the DM signal integrity capability. The output results of the CM noise voltage in the TDT are shown in Figure 9b. It can be seen that the output CM noise improves the effect. The measured data reduces the original 144 mV to 51 mV, and the improvement range is about 64.5%. This shows that the MDCRP structure filter had powerful CM noise rejection capability.



(**a**) (**b**)

Figure 9. Comparison of the measured results between the MDCRP structure filter board and the reference board. (**a**) Output voltage of the differential signal. (**b**) Output voltage of CM noise.

3.3. Eye Diagram Analysis

We then observed eye diagrams of the differential signal from the perspective of the time domain. We generated S4P files for the MDCRP structure filter board and the reference board using their measurement results. These S4P files were inputted into ADS schematic tools for eye diagram simulation. The input parameter setting generated $2^{11}-1$ pseudo-random binary sequence (PRBS), the differential signal at the input end was fed into ±0.5 V, the bit rate was 20 Gb/s, and the rise time was 10 ps.

The eye diagram simulation result of the reference board is shown in Figure 10a, and the eye diagram simulation result of the MDCRP structure filter board is shown in Figure 10b. It can be observed that the two eye diagrams of the structures show changes in their differential signals. The eye diagrams of the two structures are somewhat different, but the differential signal eye diagrams are very good for both. This proves that the addition of the MDCRP structure filter does not influence the quality of the differential signal transmission. The relevant parameters (the maximum eye height, maximum eye width, and jitter) are given in Table 2.

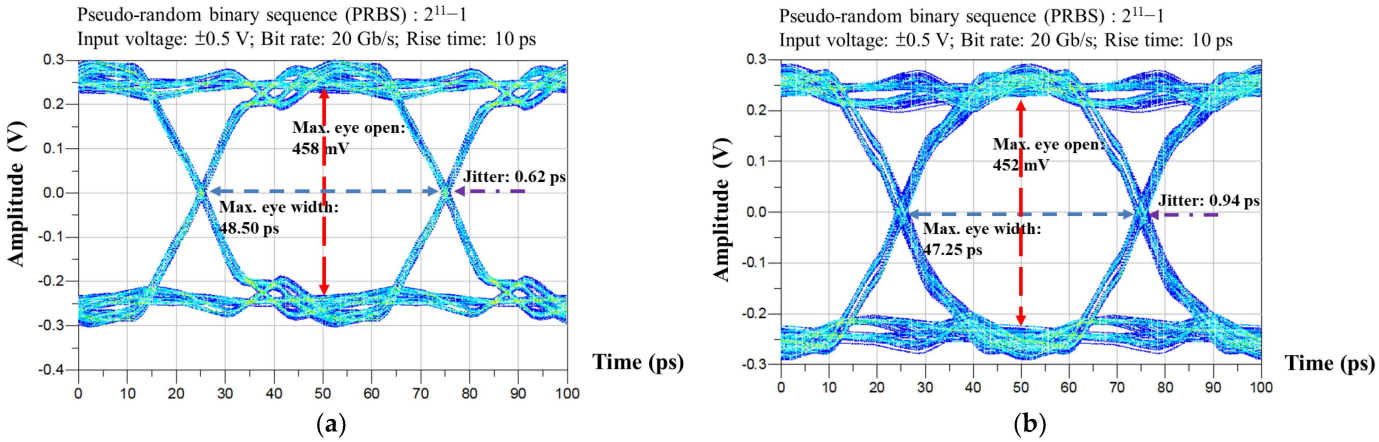


Figure 10. Eye diagram of the differential signals of the measured results. (**a**) The reference boards. (**b**) The MDCRP structure filter board.

Table 2. Comparison of the differential eye diagram parameters of the measured results.

Parameter	Max. Eye Open	Max. Eye Width	Jitter
Reference Board (20 Gb/s)	458 mV	48.50 ps	0.62 ps
MDCRP Board (20 Gb/s)	452 mV	47.25 ps	0.94 ps

It can be observed that the eye diagrams of the two structures show some differences when subjected to a numerical comparison, but both maintain good results in terms of their characteristics. This verifies once again that the MDCRP structure filter has good differential signal integrity and can maintain differential signal transmission quality. The transmission rate can reach 20 Gb/s in high-speed data transmission. These results prove that the proposed MDCRP structure filter can support HDMI 2.0 bus capabilities.

4. Discussion

Today's computer and server systems need to support high-speed transmission rate buses. A comparison of the performance of different CM noise suppression filters is shown in Table 3. It can be observed that the highest CM rejection frequency is only 10.8 GHz in the literature when using DGS structure filters. In addition, the highest CM rejection frequency is only 13.41 GHz in the literature on mushroom structure filters. Among the studied filter structures, the ring structure filter can support the highest fractional bandwidth in the literature, but the highest CM suppression frequency for a ring structure filter is only 7.87 GHz. Therefore, these different structures' filters struggle to support high-speed buses in today's computer systems.

Our novel MDCRP structure filter can support high-speed buses in today's computer and server systems. This also achieves application benefits in the industry and makes great contributions and innovations to academics. The filter size is only 0.75 λg × 0.75 λg, and the corresponding center frequency is 12.85 GHz. It can suppress CM noise at high frequencies of up to 20.62 GHz with a fractional bandwidth of up to 120.8%. The filter size and fractional bandwidth are calculated concerning the center frequency value. The MDCRP structure filter has the highest rejection bandwidth and the highest center frequency, so the filter size is the largest, and the fractional bandwidth is the worst after calculating the results.

Table 3. Comparison of the performance of different CM noise suppression filters.

Structure	Rejection Bandwidth	Center Frequency	Fractional Bandwidth	ε_r	Filter Size	PCB Layers	Year
[7]	1.52–4.07 GHz (−20 dB)	2.795 GHz	91.2%	3.5	0.43 λ_g × 0.15 λ_g	2	2015
[8]	3.7–10.8 GHz (−10 dB)	7.25 GHz	97.9%	4.4	0.3 λ_g × 0.3 λ_g	2	2016
[9]	2.9–8.1 GHz (−15 dB)	5.5 GHz	94.5%	3.27	0.36 λ_g × 0.24 λ_g	2	2019
[10]	2.75–4.6 GHz (−12.25 dB)	3.67 GHz	50.3%	3.66	0.28 λ_g × 0.18 λ_g	2	2020
[11]	3.8–7.1 GHz (−10 dB)	5.45 GHz	60.6%	—	0.16 λ_g × 0.26 λ_g	4	2010
[12]	1.65–5.2 GHz (−10 dB)	3.425 GHz	103.6%	4.5	0.11 λ_g × 0.11 λ_g	4	2012
[13]	3.53–10.1 GHz (−10 dB)	6.815 GHz	96.4%	4.4	—	3	2014
[14]	3.4–13.41 GHz (−10 dB)	8.405 GHz	119.1%	4.4	0.25 λ_g × 0.25 λ_g	5	2017
[15]	1.57–7.87 GHz (−10 dB)	4.72 GHz	133.5%	4.4	—	4	2019
[16]	5.3–10.4 GHz (−10 dB)	7.85 GHz	65.0%	4.4	2.74 λ_g × 0.55 λ_g	3	2016
[17]	3.67–17.03 GHz (−9.29 dB)	10.35 GHz	129.1%	3.09	0.60 λ_g × 0.60 λ_g	3	2023
Proposed filter	5.09–20.62 GHz (−10 dB)	12.85 GHz	120.8%	3.09	0.75 λ_g × 0.75 λ_g	3	2023

The most difficult part of our research was the geometric parameter simulation process. All geometric parameters and dependencies need to be considered, and finding the optimal configuration requires constant tuning and simulations over a long period. Another difficulty is the equivalent circuit process. The equivalent component values need to be adjusted over a long period to reach the most effective value. These efforts are all about finding the widest and best CM noise suppression effects.

Our future work will involve studying higher transmission rates exceeding 32 Gb/s to meet the design requirements of PCI Express 5.0, which will be used in future computer products. In addition, this design philosophy can be extended to the development of absorbing CM filter structures so that the whole CM filter can be designed more optimally.

5. Conclusions

This paper proposes a novel MDCRP structure filter. This uses only a three-layer PCB and can easily be embedded into PCB designs. It has good CM noise rejection performance at high frequencies while maintaining signal integrity. Additionally, it can support a transmission rate of up to 20 Gb/s, and the eye diagram is a good performance in the measured. The MDCRP structure filter can support HDMI 2.0, PCI Express 4.0, USB 3.2, and SATA Express, meaning that it meets the design needs of current computer and server products.

Author Contributions: Conceptualization, C.-K.Y., D.-B.L. and H.-P.L.; methodology, C.-K.Y. and D.-B.L.; software, C.-K.Y.; validation, C.-K.Y.; formal analysis, C.-K.Y.; investigation, C.-K.Y.; resources, D.-B.L. and H.-P.L.; data curation, C.-K.Y.; writing—original draft preparation, C.-K.Y.; writing—review and editing, C.-K.Y.; visualization, C.-K.Y.; supervision, D.-B.L.; project administra-

tion, D.-B.L. and H.-P.L.; funding acquisition, D.-B.L. and H.-P.L. All authors have read and agreed to the published version of the manuscript.

Funding: This work was supported by National Taiwan University of Science and Technology, Taipei, Taiwan.

Institutional Review Board Statement: Not applicable.

Informed Consent Statement: Not applicable.

Data Availability Statement: Not applicable.

Conflicts of Interest: The authors declare no conflict of interest.

References

1. Bogatin, E. *Signal and Power Integrity—Simplified*, 2nd ed.; Pearson Education: Boston, MA, USA, 2010.
2. Hall, S.H.; Heck, H.L. *Advanced Signal Integrity for High-Speed Digital Designs*; Wiley: Hoboken, NJ, USA, 2009.
3. Montrose, M.I. *Printed Circuit Board Design Techniques for EMC Compliance—A Handbook for Designers*, 2nd ed.; IEEE Press: New York, NY, USA, 2000.
4. Sharawi, M.S. Practical issues in high speed PCB design. *IEEE Potentials* **2004**, *23*, 24–27. [CrossRef]
5. Fornberg, P.E.; Kanda, M.; Lasek, C.; Piket-May, M.; Hall, S.H. The impact of a nonideal return path on differential signal integrity. *IEEE Trans. Electromagn. Compat.* **2002**, *44*, 11–15. [CrossRef]
6. Shiue, G.-H.; Shiu, J.-H.; Tsai, Y.-C.; Hsu, C.-M. Analysis of common-mode noise for weakly coupled differential serpentine delay microstrip line in high-speed digital circuits. *IEEE Trans. Electromagn. Compat.* **2012**, *54*, 655–666. [CrossRef]
7. Zhu, H.-R.; Mao, J.-F. An ultra-wideband common-mode suppression filter based on S-DBCSRR for high-speed differential signals. *IEEE Microw. Wirel. Compon. Lett.* **2015**, *25*, 226–228. [CrossRef]
8. Lin, D.-B.; Lee, Y.-H. A wideband common-mode suppression filter using enhanced coupled defected ground structure. In Proceedings of the 2016 IEEE International Symposium on Electromagnetic Compatibility (EMC), Ottawa, ON, Canada, 25–29 July 2016; pp. 791–796.
9. Zeng, Z.; Chen, S.J.; Fumeaux, C. A reconfigurable filter using defected ground structure for wideband common-mode suppression. *IEEE Access* **2019**, *7*, 36980–36990. [CrossRef]
10. Savitha, R.; Karuppiah, V. Dual resonant DGS based common-mode filter for high-speed digital circuit applications. In Proceedings of the 2020 International Conference on Communication and Signal Processing (ICCSP), Chennai, India, 28–30 July 2020; pp. 76–78.
11. Tsai, C.-H.; Wu, T.-L. A Broadband and Miniaturized Common-Mode Filter for Gigahertz Differential Signals Based on Negative-Permittivity Metamaterials. *IEEE Trans. Microw. Theory Tech.* **2010**, *58*, 195–202. [CrossRef]
12. Hsiao, C.-Y.; Tsai, C.-H.; Chiu, C.-N.; Wu, T.-L. Radiation Suppression for Cable-Attached Packages Utilizing a Compact Embedded Common-Mode Filter. *IEEE Trans. Compon. Packag. Manuf. Technol.* **2012**, *2*, 1696–1703. [CrossRef]
13. Shiue, G.-H.; Hsu, C.-M.; Yeh, C.-L.; Hsu, C.-F. A Comprehensive Investigation of a Common-Mode Filter for Gigahertz Differential Signals Using Quarter-Wavelength Resonators. *IEEE Trans. Compon. Packag. Manuf. Technol.* **2012**, *4*, 134–144. [CrossRef]
14. Lin, D.-B.; Chen, Y.-C.; Wu, C.-T. A broadband filter design for common-mode noise suppression with multilayer mushroom structure in differential transmission line. In Proceedings of the 2017 IEEE International Symposium on Electromagnetic Compatibility & Signal/Power Integrity (EMCSI), Washington, DC, USA, 7–11 August 2017; pp. 310–314.
15. Lin, D.-B.; Chen, Y.-H.; Zheng, Y.-H.; Chen, B.-Y. A Broadband Common Mode Filter With Embedded Ring Structure. In Proceedings of the 2019 Joint International Symposium on Electromagnetic Compatibility, Sapporo and Asia-Pacific International Symposium on Electromagnetic Compatibility (EMC Sapporo/APEMC), Sapporo, Japan, 3–7 June 2019; pp. 379–382.
16. Kim, M. Periodically corrugated reference planes for common-mode noise suppression in high-speed differential signals. *IEEE Trans. Electromagn. Compat.* **2016**, *58*, 619–622. [CrossRef]
17. Yu, C.-K.; Lin, D.-B.; Lin, H.-P. Wideband common-mode suppression filter using defected corrugated reference plane structures. *Microw. Opt. Technol. Lett.* **2023**. [CrossRef]

Disclaimer/Publisher's Note: The statements, opinions and data contained in all publications are solely those of the individual author(s) and contributor(s) and not of MDPI and/or the editor(s). MDPI and/or the editor(s) disclaim responsibility for any injury to people or property resulting from any ideas, methods, instructions or products referred to in the content.